Synthetic and Systems Biotechnology 10 (2025) 835–845

Contents lists available at ScienceDirect

Synthetic and Systems Biotechnology

journal homepage: www.keaipublishing.com/en/journals/synthetic-and-systems-biotechnology

Original Research Article

Enhanced L-serine synthesis in *Corynebacterium glutamicum* by exporter engineering and Bayesian optimization of the medium composition

Yifan Huang [a], Yujie Gao [b], Yamin Huang [a], Xiaogang Wang [d], Meijuan Xu [b], Guoqiang Xu [b], Xiaojuan Zhang [b], Hui Li [a], Jinsong Shi [a], Zhenghong Xu [c], Xiaomei Zhang [a,*]

[a] Laboratory of Pharmaceutical Engineering, School of Life Science and Health Engineering, Jiangnan University, Wuxi, 214122, Jiangsu, China
[b] Biotechnology of Ministry of Education, School of Biotechnology, Jiangnan University, Wuxi, 214122, Jiangsu, China
[c] College of Biomass Science and Engineering, Sichuan University, Chengdu, 610065, Sichuan, China
[d] Key Laboratory of Advanced Control for Light Industry Processes, Ministry of Education, Jiangnan University, Wuxi, 214122, Jiangsu, China

ARTICLE INFO

Keywords:
Corynebacterium glutamicum
L-serine
Exporter
Semi-rational design
Bayesian optimization

ABSTRACT

L-serine is a versatile, high value-added amino acid, widely used in food, medicine and cosmetics. However, the low titer of L-serine has limited its industrial production. In this study, a cell factory without plasmid for efficient production of L-serine was constructed based on transport engineering. Firstly, the effects of L-serine exporter SerE overexpression and deletion on the cell growth and L-serine titer were investigated in *Corynebacterium glutamicum* (*C. glutamicum*) A36, overexpression of *serE* using a plasmid led to a 15.1% increase in L-serine titer but also caused a 15.1% decrease in cell growth. Subsequently, to increase the export capacity of SerE, we conducted semi-rational design and bioinformatics analysis, combined with alanine mutation and site-specific saturation mutation. The mutant E277K was obtained and exhibited a 53.2% higher export capacity compared to wild-type SerE, resulting in L-serine titer increased by 39.6%. Structural analysis and molecular dynamics simulations were performed to elucidate the mechanism. The results showed that the mutation shortened the hydrogen bond distance between the exporter and L-serine, enhanced complex stability, and reduced the binding energy. Finally, Bayesian optimization was employed to further improve L-serine titer of the mutant strain C-E277K. Under the optimized conditions, 47.77 g/L L-serine was achieved in a 5-L bioreactor, representing the highest reported titer for *C. glutamicum* to date. This study provides a basis for the transformation of L-serine export pathway and offers a new strategy for increasing L-serine titer.

1. Introduction

L-serine is a high value-added amino acid, widely used in food, medicine and cosmetics, with great market prospects [1]. Currently, L-serine production mainly depends on protein hydrolysis extraction, chemical synthesis, or conversion from precursor [2,3]. However, these methods suffer from high costs, low conversion rates, and environmental pollution, prompting the search for new green production methods for L-serine [4]. Direct fermentative production of L-serine from sugars has attracted increasing attention, and has been performed in engineered *Escherichia coli* (*E. coli*) [5,6] and *Corynebacterium glutamicum* (*C. glutamicum*) [7,8]. Rennig constructed a recombinant *E. coli* that could produce L-serine by fermentation from glucose, and the L-serine titer reached 50 g/L after fed-batch fermentations [9], representing the highest reported titer for *E. coli* to date. In *C. glutamicum*, Zhang et al. overexpressed *serE* and the key L-serine synthesis enzymes *serA*Δ197, *serC* and *serB*, and the resulting strain produced 43.9 g/L L-serine using sucrose as carbon source [10]. Compared with *E. coli*, *C. glutamicum* is a native amino acid secretion strain for L-serine production using in food and pharmaceutical fields [11].

At present, strategies to increase L-serine titer in *C. glutamicum* mainly focus on enhancing its biosynthesis and inhibiting its degradation pathway, however, the L-serine titer remains relatively low. Since the export systems of strain are usually related to the amino acid excretion, engineering exporters is a useful strategy for improving strains [12,13]. For example, by overexpressing L-lysine exporter LysE in *C. glutamicum* S9114, L-ornithine titer was increased by 18.4 g/L [14]. Plasmids are usually used to overexpress exporters, but their presence of

Peer review under the responsibility of Editorial Board of Synthetic and Systems Biotechnology.
* Corresponding author. Lihu Avenue No. 1800, Jiangnan University, Wuxi, 214122, China.
E-mail address: zhangxiaomei@jiangnan.edu.cn (X. Zhang).

https://doi.org/10.1016/j.synbio.2025.04.003
Received 13 January 2025; Received in revised form 3 April 2025; Accepted 6 April 2025
Available online 9 April 2025

plasmids imposes a metabolic burden on the strain and leads to batch-to-batch fermentation variations. In our laboratory, it has been found that SerE is the main exporter of L-serine [10,15], and enhancing export by modifying SerE is an important method to increase L-serine titer.

Medium optimization is a necessary step to improve L-serine titer. However, biological system is complex, and cell growth and production are affected by many factors, making it difficult to determine the optimal growth conditions. Factorial design and artificial neural network were usually used to seek an optimal setting for obtaining a high yield. The former demands a strict design structure of the input, and the number of test runs increases exponentially as the dimensionality of the input increases [16]. The latter also requires a large amount of data to train the network and re-structure itself to avoid overfitting [17]. In contrast, Bayesian optimization adopts an inherently adaptive strategy, using a probabilistic surrogate model and acquisition function to dynamically guide experiments [18]. This allows Bayesian optimization to efficiently determine the best solution with minimal experimental effort. Therefore, Bayesian optimization is a quick and cost-efficient alternative to determine optimal settings of fermentation.

In this study, the effects of L-serine exporter SerE on cell growth and L-serine titer were investigated firstly. Then, a semi-rational design strategy was used to modify the exporter SerE through computer aided design and bioinformatics analysis, and a mutant library was constructed to screen for mutants with improved export ability. The reason for the higher export ability of the mutants were analyzed through structure analysis and molecular dynamics simulation. Finally, to increase the L-serine further, Bayesian optimization was performed on the mutant strain. This study provides a new idea for increasing L-serine titer.

2. Materials and methods

2.1. Strains and plasmids

All the strains and plasmids used in this study are listed in Table 1. In this study, *C. glutamicum* A36 was used as the parent strain for generating the mutant strains, and *E. coli* JM109 was used as a host for plasmid construction.

2.2. Medium and growth conditions

C. glutamicum was cultured in seed medium (per liter: 20.0 g glucose, 37.0 g Brain Heart Infusion, 10.0 g $(NH_4)_2SO_4$, 0.5 g $MgSO_4{\cdot}7H_2O$, 0.3 g NaH_2PO_4, and 0.2 g K_2HPO_4) overnight to an optical density (OD_{562}) of about 25 in orbital shaker at 30 °C with shaking at 120 rpm. Then, 1 mL

Table 1
Strains, plasmids and primers used in this study.

Strain/plasmid/primer	Genotype or description	Sources or reference
Strain		
E. coli		
JM109	*recA1*, *endA1*, *gyrA96*, *thi-1*, *hsd R17* (rk^-mk^+) *supE4*	Invitrogen
C. glutamicum		
SSAAI	*C. glutamicum* SYPS-062-33a with deletion of the 591 bp in the C-terminus of *serA*, deletion of *sdaA*, *alaT*, *avtA*, and attenuation of *ilvBN*	CGMCC No.15170
A36	A mutant of *C. glutamicum* SSAAI was obtained by Fluorescence-Activated Cell Sorting (FACS) after atmospheric and room temperature plasma (ARTP) mutagenesis	CGMCC No.15171
A36Δ*serE*	*C. glutamicum* A36 with additional deletion of *serE*	This study
A36-*serE*	*C. glutamicum* A36 with overexpression of *serE*	This study
pD-I158A	*C. glutamicum* A36 with plasmid pDXW-10-*serE*-I158A	This study
pD-S161A	*C. glutamicum* A36 with plasmid pDXW-10-*serE*-S161A	This study
pD-Y218A	*C. glutamicum* A36 with plasmid pDXW-10-*serE*-Y218A	This study
pD-E221A	*C. glutamicum* A36 with plasmid pDXW-10-*serE*-E221A	This study
pD-E240A	*C. glutamicum* A36 with plasmid pDXW-10-*serE*-E240A	This study
pD-E277A	*C. glutamicum* A36 with plasmid pDXW-10-*serE*-E277A	This study
pD-K280A	*C. glutamicum* A36 with plasmid pDXW-10-*serE*-K280A	This study
C-E277H	*C. glutamicum* A36 with Glu-277→His mutation in *serE*	This study
C-E277K	*C. glutamicum* A36 with Glu-277→Lys mutation in *serE*	This study
C-E277M	*C. glutamicum* A36 with Glu-277→Met mutation in *serE*	This study
Plasmid		
pDXW-10 (pD)	*E. coli-C. glutamicum* shuttle vector, *tacM* promoter, Km^r	[53]
pK18mob*sacB*	Integration vector, *oriV*, *oriT*, mob, *sacB*, Km^r	[21]
pDXW-10-*serE*	pDXW-10 containing *serE*	This study
pK18mob*sacB*-*serE*	vector for deletion of *serE*	This study
pK18mob*sacB*-E277K	pK18mob*sacB* with Glu-277→Lys mutation in *serE*	This study
Primer	Sequences (5′–3′)	
SerE-1	ctatgacatgattac**gaattc**AGTTCTTCGAGCGCTGCGG (*Eco*RI)	This study
SerE-2	ctgcacgttaaGCCCTTGATTATTGCCAAAGAA	This study
SerE-3	atcaagggcTTAACGTGCAGGCTTACCTTTTG	This study
SerE-4	tgcctgcaggtcgac**tctaga**CACATGATGCGTACCGGTGC (*Xba*I)	This study
pDXW-10-*serE*-F	ttcacacaggaaaca**gaattc**TTGAGATTGAGCACGACACC (*Eco*RI)	This study
pDXW-10-*serE*-R	catccgccaaaacag**aagctt**CTAGGTGTGTGTACTCGCCTC (*Hin*dIII)	This study
S161-F	ATCCTGGCANNKAAGAAAATCGGCCAACTCATCCCC	This study
S161-R	GATTTTCTTMNNTGCCAGGATGTAGCACACCCAGAA	This study
E221-F	CTATTCGCTGNNKTTATCGGCACTG	This study
E221-R	GATAAMNNCAGCGAATAGGGGATAAGCG	This study
E240-F	CTCAGCCTCNNKCCGGCATTCGCCGCCGCCGTCGGC	This study
E240-R	GAATGCCGGMNNGAGGCTGAGCAGAATGCTGAAAAT	This study
E277-F	ACGTGGNNKCCTAAAAAGATGCTTGT	This study
E277-R	TTTAGGMNNCCACGTGACGCCGAT	This study
K280-F	CCTAAANNKATGCTTGTCGACGCG	This study
K280-R	AAGCATMNNTTTAGGCTCCCACGTGA	This study

of the bacterial solution was inoculated into a 250 mL flask containing 25 mL of the fermentation medium (per liter: 100.0 g sucrose, 30.0 g $(NH_4)_2SO_4$, 3.0 g KH_2PO_4, 0.5 g $MgSO_4{\cdot}7H_2O$, 20 mg $FeSO_4{\cdot}7H_2O$, 20 mg $MnSO_4{\cdot}H_2O$, 60.0 g $CaCO_3$, 30 mg protocatechuic acid (PCA), 50 μg biotin, and 450 μg thiamine) so that the initial OD_{562} = 1. The fermentation medium was incubated at 30 °C and 120 rpm for 120 h, and samples were taken periodically to determine the concentration of amino acids, biomass and sugars. *E. coli* JM109 was grown in lysogeny broth (LB) medium (per liter: 5 g yeast extract, 10 g tryptone, and 10 g NaCl) at 37 °C with shaking at 220 rpm for 12 h. When appropriate, ampicillin (100 mg/L) or kanamycin (50 mg/L) was added to the medium. 5-L bioreactor (Korea Co., Ltd., KF-5 L) was used for large volume L-serine production with an effective working volume of 2.5 L. Temperature and pH were kept at 30 °C and 7, respectively. The dissolved oxygen level was kept constant at 15% by controlling the stirrer speed and aeration rate. The fermentation time was 120 h. Other parameters refer to previous studies [11].

2.3. Construction of strains

The primers and restriction endonucleases used for plasmid construction in this study are shown in Table 1. The plasmid was amplified by PCR using the chromosomal DNA of *C. glutamicum* A36 as a template, and the isolation of plasmids from *E. coli* was performed using plasmid mini-preps kits according to the protocol from Generay (Shanghai). The preparation of competent cells were performed according to the published methods [19]. The *serE* gene was overexpressed in *C. glutamicum* using the shuttle expression plasmid pDXW-10 [20], which was digested with *Eco*RI and *Hin*dIII and ligated with the plasmid pDXW-10 with the corresponding cleavage site to construct pDXW-10-*serE*.

The non-replicable integrating plasmid pK18mob*sacB* was utilized to delete DNA sequences in *C. glutamicum* [21]. Destroying DNA sequences in *C. glutamicum* was achieved by homologous recombination technology. The *in vitro* homologous recombinant seamless cloning reagents was purchased from Takara (Beijing). The procedure for deleting gene *serE* is hereby detailed for example. First, primers SerE-1/SerE-2 and SerE-3/SerE-4 were used to amplify the upstream and downstream DNA fragments of *serE*. Plasmid pK18mob*sacB* which was digested by *Xba*I and *Hin*dIII, and then joined with a fragment of DNA which fused two corresponding arms of *serE*. After that, the recombinant plasmid with the DNA for targeting was introduced into *C. glutamicum* A36 by Micro-Pulser Electroporator (Bio-Rad Laboratories, Inc.) [21]. Finally, the transformants were verified by PCR after growing in 10% sucrose screening medium for 72 h at 30 °C.

2.4. Mutagenesis of SerE

2.4.1. Saturation mutagenesis of SerE

SerE was subjected to saturation mutagenesis using mutant primers at different sites in Table 1. The procedure for $SerE^{E277A}$ mutation is hereby detailed for example. First, reverse PCR was performed on the DNA of shuttle plasmid pDXW-10-*serE* and non-replicable deletion plasmid pK18mob*sacB*-*serE*, and glutamate at site 277 in SerE was replaced with alanine. Next, the purified PCR products were recovered after digestion of the plasmid DNA with *Dpn*I. The PCR products are linked by homologous recombinase and transformed in *E. coli*, and the mutation sites were verified by sequencing. Finally, the electric transformation method and strain verification method were consistent with the knockout strain construction method.

2.4.2. Computer simulated mutation of SerE

Based on the basic structure of SerE, Rosetta [22] was used to simulate the transition from wild type to mutant protein at each site, and the free energy of unfolding (ΔG) during the transition was calculated to determine the stability of the protein before and after mutation.

2.5. L-serine export capacity determination

To determine the L-serine export capacity of SerE, the classical amino acid export assay was used for export capacity determination [23]. In brief, when the preincubated cells grew to logarithmic growth stage, they were washed twice with CGXII minimal medium (per liter: 40.0 g glucose, 5.0 g urea, 20.0 g $(NH_4)_2SO_4$, 1.0 g KH_2PO_4, 1.0 g K_2HPO_4, 0.25 mg $MgSO_4$, 42.0 g MOPS, 10 mg CaCl, 10 mg $FeSO_4{\cdot}7H_2O$, 10 mg $MnSO_4{\cdot}H_2O$, 1 mg $ZnSO_4$, 0.2 mg $CuSO_4$, 0.02 mg $ZiCl_2{\cdot}6H_2O$, 30 mg PCA, 0.2 mg biotin) [24], inoculated into 50 mL of CGXII minimal medium containing 3 mM Ser-Ser (L-serine dipeptide, Nanjing Peptide Industry Co., LTD.) and incubated for 2 h at 30 °C, 120 rpm. After the pre-culture, the cells were harvested again, and washed twice with cold CGXII minimal medium [25]. The initial cell concentration of OD_{562} was controlled to be 8–10, and inoculated into 50 mL/500 mL CGXII minimal medium. Amino acid export was initiated by the addition of 3 mM Ser-Ser and samples were taken every 15 min and the concentration of amino acids was determined by HPLC (1260 Infinity III, Agilent) [26].

2.6. Homology modeling and molecular docking analysis

The 3D structure models of the studied proteins were predicted using Alphafold 2 (https://alphafold.com) [27]. Substrates were docked into the structure of SerE using Autodock 4.0 equipped with ADT for hydrogenation and energy minimization after all waters were removed [28]. Semi-flexible docking was performed and other parameters were kept at default values. The top 10 lowest energy docking poses of the substrates from all search results were selected, among which the ideal conformations were chosen for further analysis.

2.7. Combined free energy calculation and molecular dynamics simulation

The MD simulation was conducted using the AMBER 18 [29] program under constant temperature, pressure and periodic boundary conditions. The GAFF2 small molecule force field was used for small molecules and similarly proteins were treated using the ff14SB protein force field [30,31], after which hydrogen atoms were added to the system, the composite system was placed in a solvent cartridge and Na^+/Cl^- was added to the system for balancing the system charge. In the MD simulation process, the Coulomb interaction was truncated to 10 Å [32]. The Langevin was used to control the simulated temperature to 298.15 K, and the system pressure was 1 atm. NVT and NPT balance simulation was performed at 298.15 K. Finally, a 100 ns MD simulation was performed on the composite system, with conformations saved every 10 ps, and the visualization of the simulation results was completed using Pymol [33].

2.8. Analytical procedures

The cell density was measured as the absorbance value at a wavelength of 562 nm (OD_{562}) by UV–VIS spectrophotometer (AOE Instruments Co. Inc., Shanghai, China). The determination methods of sucrose content and L-serine titer in fermentation process refer to previous studies [34].

2.9. Statistical analysis

GraphPad Prism 8.0 Software and Origin 2018 Software was used to draw column line charts. The data were presented in tables and figures in the form of mean values and standard deviations, and all experiments were conducted in triplicate. A probability (p) value < 0.05 was considered statistically significant.

2.10. Bayesian optimization

Twenty settings of medium were randomly generated (X) and tested (Y) for the initial data collection (Table 4). Then, a Gaussian process regression was conducted to predict the mean and variance of the unknown input x:

$\mu(x), \sigma(x) = GP(X, Y, \sigma_f, l)$, where σ_f, l are hyperparameters estimated by maximizing the likelihood $p(Y|X, \sigma_f, l)$.

Then a search for promising candidates (X^*) was executed by optimizing probability of improvement:

$X^* = argmax\, p[\mu(x) \geq y^* + \xi]$, where y^* is the known highest yield and ξ is a trade-off coefficient which was empirically assigned with [100,1, 0.02, 0, −0.02, −1, −100] to obtain the extremes of the function in this study. Similar candidates were compared, and only the unique ones were retained. After testing the candidates, the dataset (X, Y) was renewed, and the procedure continued until no improvements were observed anymore. All the optimization problems mentioned in this section were solved by a genetic algorithm, and the method was shown in our previous study [35].

3. Results

3.1. Effects of SerE overexpression or deletion on the cell growth and L-serine titer

In order to investigate the effect of SerE on cell growth and L-serine titer, we overexpressed and deleted *serE* in *C. glutamicum* A36 (A36), and constructed *serE* overexpression strain *C. glutamicum* A36-*serE* (A36-*serE*) and *serE* deletion strain *C. glutamicum* A36Δ*serE* (A36Δ*serE*). As shown in Fig. 1A, during 0–24 h, strain A36Δ*serE* grew fastest in the three strains, followed by strain A36 and A36-*serE*. At the end of fermentation, the cell growth of *serE* overexpression strain (A36-*serE*) and *serE* deletion strain (A36Δ*serE*) was 15.1% and 14.2% lower than that of the parent strain A36, respectively. Compared with strain A36, the specific growth rate of A36Δ*serE* increased rapidly before fermentation for 24 h, and the cell growth rate decreased after 24 h. However, the strain A36-*serE* harboring the plasmid grew slowly before fermentation for 24 h, and then showed similar cell growth rate as strain A36 (Fig. 1B). Strikingly, A36Δ*serE* produced 6.56 g/L L-serine, which was 78.2% lower than that of the parent strain A36 (Fig. 1C). However, plasmid-borne overexpression of SerE compensated for the lack of SerE with respect to L-serine titer, resulting in 34.71 g/L L-serine, which was 15.1% higher than that of the parent strain A36. These results suggest that SerE may have some effect on cell growth and play an important role in the export of L-serine.

Further, L-serine export capacity of SerE was evaluated using peptide feeding approach in strain A36, *serE* overexpression strain (A36-*serE*) and *serE* deletion strain (A36Δ*serE*) respectively. 3 mM dipeptides were added to the medium, and the extracellular L-serine concentrations were determined by HPLC. The results revealed that L-serine concentration was comparable among the three strains and had not significantly change before 45 min (Fig. 1D). After 45 min, the L-serine concentration of strain A36-*serE* was significantly increased due to SerE overexpression. When reaching 120 min, L-serine concentration of A36-*serE* were increased by 15.5% compared to A36. Due to the absence of SerE, the export speed of L-serine was slower in A36Δ*serE*. When reaching 120 min, L-serine concentrations of A36Δ*serE* were reduced by 43% compared to A36. These results suggest that SerE overexpression

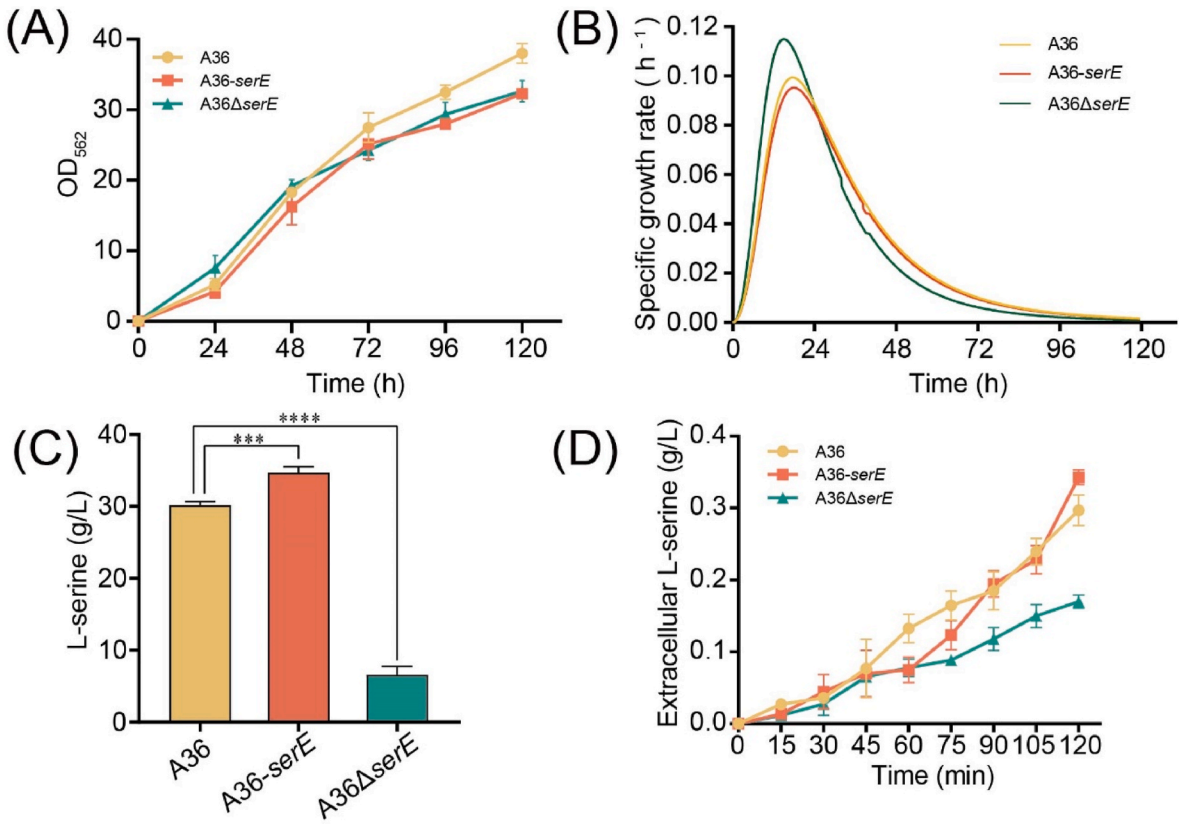

Fig. 1. The effect of SerE overexpression and deletion to the cell growth and L-serine titer. (A) The cell growth (OD_{562}) of strain A36 (yellow), A36-*serE* (red) and A36Δ*serE* (cyan). (B) Growth rates of strain A36 (yellow), A36-*serE* (red) and A36Δ*serE* (cyan). (C) The L-serine titer of strain A36 (yellow), A36-*serE* (red) and A36Δ*serE* (cyan). (D) Amino acid export assays of strain A36 (yellow), A36-*serE* (red) and A36Δ*serE* (cyan). All data are averages of three independent experiments, and the error bars represent the standard deviation of biological replicates. Statistical analysis was performed with the two-tailed unpaired Student's *t*-test (*$p < 0.05$, **$p < 0.01$, ***$p < 0.001$, ****$p < 0.0001$).

enhanced L-serine export, then L-serine titer increased.

3.2. Biological information of SerE and identifying of mutation sites

Plasmid-based overexpression of SerE can increase L-serine titer, but it affects cell growth. To increase L-serine titer by improving the export efficiency of SerE is very important. AlphaFold 2 is a deep learn-based method for protein structure prediction, which has become an important tool for predicting three-dimensional protein structure. Due to the lack of studies on the protein structure of SerE, to identify the binding site of L-serine and SerE, AlphaFold 2 was first used to model the protein structure of SerE (Fig. 2A). It can be seen that SerE is a monomer. It is reported that the spatial configuration of the exporter and the interactions between the substrate and the protein play a key role in determining the export capacity of the exporter. Therefore, to evaluate the accuracy of the model, SAVES 6.0 website was used to evaluate the modeling results, and Ramachandran plot tool is used to analyze the SerE homology modeling results. The results showed that 91.4% (>90%) of amino acid residues in the constructed protein model were located in the optimal rational region, indicating that the model had good reliability (Fig. 2B).

The binding sites of L-serine and SerE were searched through the molecular docking between the exporter and the small molecule ligand. Residues E277 and K280 were found to establish hydrogen bonds with hydroxyl and amino groups of ligands (Fig. 2C). Meanwhile, through Rosetta calculation and simulation prediction results (Table 2), five loci with large changes in free energy were selected. Therefore, the mutation loci of SerE were finally identified as Ile158, Ser161, Pro218, Glu221, Glu240, Glu277 and Lys280 by the two strategies. In order to further clarify the influence of these seven mutation sites on L-serine export, TMHMM Server v.2.0 software was used to predict the transmembrane helical structure of SerE. As can be seen from Fig. 2D, the SerE has 10 alpha-helix transmembrane segments with the N-terminal and C-terminal located on the same side. Ile158 and Pro218 are located in the transmembrane region of the export protein, while Ser161, Glu221, Glu240, Glu277 and Lys280 are located in different helical transmembrane segments. In general, we clarified the three-dimensional structure of SerE through modeling, and found seven sites that may affect the L-serine export of SerE.

Table 2
Selection of pseudo-mutant amino acids.

Site	Amino acid	Rosetta value
Ile	158	−2.0
Ser	161	−5.26
Tyr	218	−2.59
Glu	221	−4.0
Glu	240	−5.95

Rosetta value is the change of folding free energy ΔG (kcal/mol).

3.3. Screening SerE variants to facilitate L-serine production

To further explore the role of these residues in the export of L-serine, alanine mutations were used to screen key sites firstly. Amino acids at seven sites (Ile158, Pro218, Ser161, Glu221, Glu240, Glu277 and Lys280) of SerE were individually mutated to alanine, and the L-serine titer of each mutant was determined. The strain with SerE

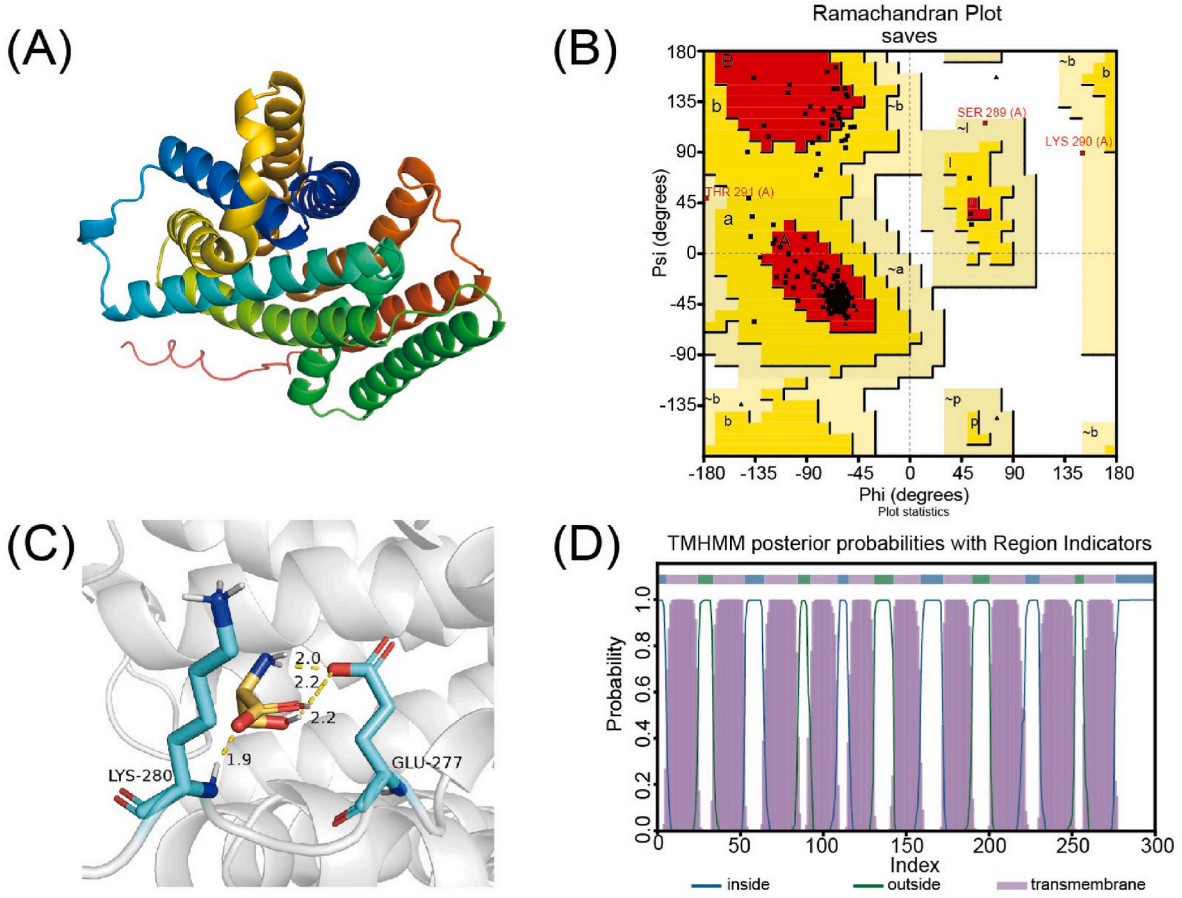

Fig. 2. Biological information of SerE and identification of mutation sites. (A) AlphaFold prediction of SerE 3D structure. (B) SerE 3D structural model evaluation (red: optimal rational zone, Yellow: add reasonable area, Light yellow: general reasonable area). (C) Docking of L-serine with SerE. (D) SerE transmembrane region prediction (blue: inside, green: outside, pink: transmembrane).

overexpression (A36-*serE*) was used as a control. As shown in Fig. 3A, five mutants (S161, E221, E240, E277 and K280) exhibited higher L-serine titer compare to strain A36-*serE*. Based on these results, saturation mutagenesis was performed at these five sites in strain A36-*serE* for further screening, resulting in a total of 95 mutants.

The distribution of L-serine titer in five sites of saturation mutant strains was analyzed. As shown in Fig. 3B, at the plasmid level, all saturated mutations at site E277 and K280 led to an increase in L-serine titer compared to the other three sites (Fig. 3C). Compared to the parent strain A36, L-serine titer of saturation mutant strains at S161, E221 and E240 was lower or had little change, while L-serine titer of all mutant strains at E277 and K280 was higher than that of the strain A36. The L-serine titer of the four mutant strains at E277 site increased by more than 10% compared to the parent strain, with the mutant strain pD-E277K achieving the highest L-serine titer of 40.17 g/L, representing a 15.7% higher than that of strain A36-*serE*.

In addition, the L-serine titer of the K280 mutant strain pD-K280D was 11.8% higher than that of A36-*serE*. These results indicated that mutations at E277 and K280 had significant effect on L-serine titer, suggesting that E277 and K280 sites may be key sites for SerE binding to L-serine. To further verify the role of these two sites, saturation mutations at E277 and K280 sites were subsequently performed at the genomic level.

3.4. The effect of SerE mutation to the L-serine production

The SerE of strain A36 was mutated by single point saturation mutation at E277 and K280, resulting in the 38 recombinant strains. The fermentation results showed that the L-serine titer of mutant strains C-E277H (34.79 g/L), C-E277K (42.09 g/L), and C-E277M (36.82 g/L) was 15.4%, 39.6% and 22.1% higher than that of the parent strain A36 (30.15 g/L) respectively (Fig. 4A). In contrast, the L-serine titer of the other mutant strains showed little difference compared to the parent strain (Fig. 4B). Based on these results, the mutant C-E277K was selected for further study.

To elucidate the reasons for the increase of L-serine titer of mutant C-E277K, amino acid export experiment was conducted. Different concentrations of Ser-Ser were added to the cultures of C-E277K and A36, and the L-serine concentration were compared. When 4 mM Ser-Ser was added, the export capacity of mutant C-E277K continued to increase, resulting in an L-serine concentration was 53.2% higher than that of A36 at 120 min (Fig. 4C). Moreover, as shown in Fig. 4D, mutant C-E277K excreted L-serine at a higher rate than the parent strain A36 at 120 min, suggesting that SerE^{E277K} had a higher L-serine export activity than SerE.

To analyze the molecular mechanisms of the SerE^{E277K} enhancing L-serine export, the interaction of the SerE, SerE^{E277K} and L-serine ligands were analyzed (Fig. 5A). The hydrogen bond distances between mutant SerE^{E277K} and L-serine were found to be shorter compared to the wild type SerE, likely due to stronger interactions between the mutant and L-serine, which facilitated increased export. Additionally, the local surface charge at position 277 of mutant SerE^{E277K} changed from strongly negative (glutamate) to strongly positive (lysine) (Fig. 5B). This change in charge distribution aligned with the surrounding electrostatic potential, suggesting that the mutation led to favorable alterations in surface electrostatics, thereby stabilizing the SerE^{E277K} protein.

A 100 ns MD simulation was performed to compare the stability of SerE and its mutant SerE^{E277K} (Fig. 5C). A smaller root mean square deviation (RMSD) value usually indicates that the molecular structure is more stable during the simulation. The results showed that the mutant SerE^{E277K} reached equilibrium after 20 ns, with an average RMSD value

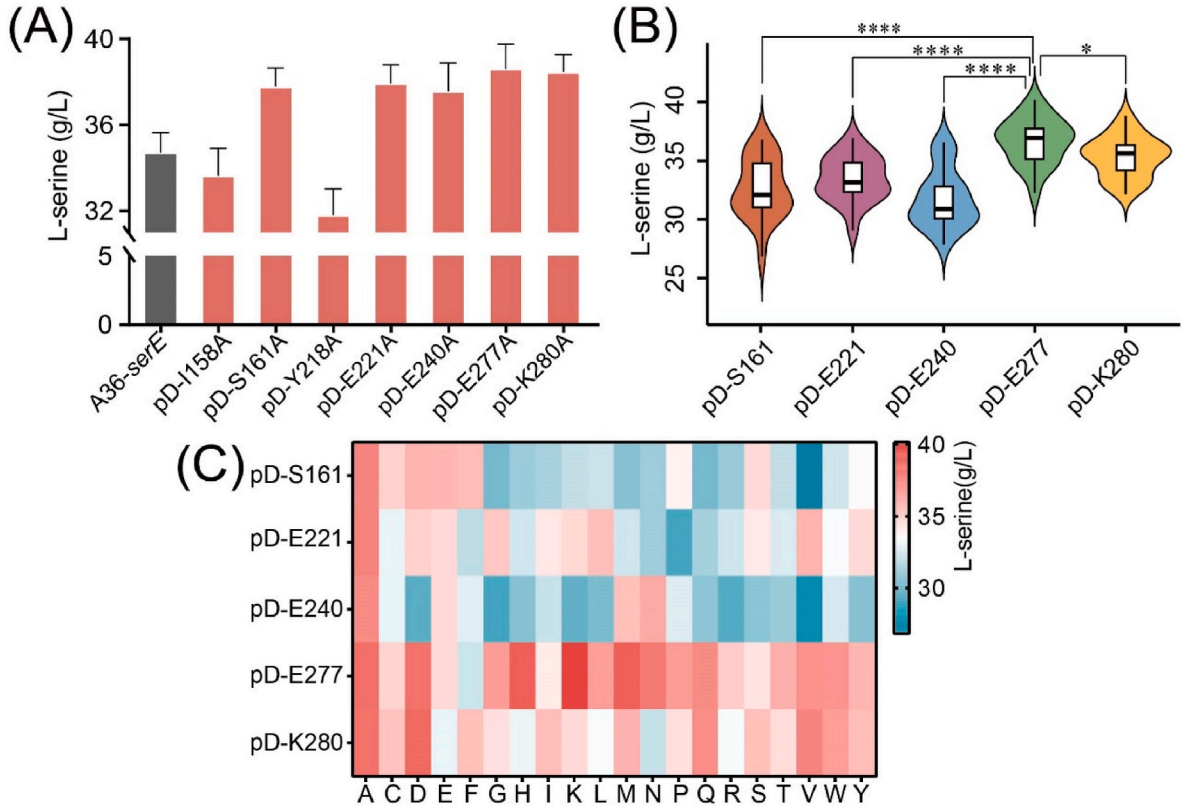

Fig. 3. Screening of SerE mutants. (A) Mutation sites with increased L-serine titer were screened. Seven sites of SerE were mutated to alanine, and L-serine titers of A36-*serE* and mutant strains were determined. (B) L-serine titers of saturation mutants at five sites. The selected sites were mutated into 19 other amino acids, and the L-serine titer of the mutant strains was determined. (C) L-serine titer was visualized by a heatmap. The color key indicates the L-serine titer of the mutant. pD-S161, pD-E221, pD-E240, pD-E277 and pD-K280 represent the S161, E221, E240, E277 and K280 sites at the plasmid level, respectively, and these symbols do not represent a single strain, but refer to all mutant strains at that site.

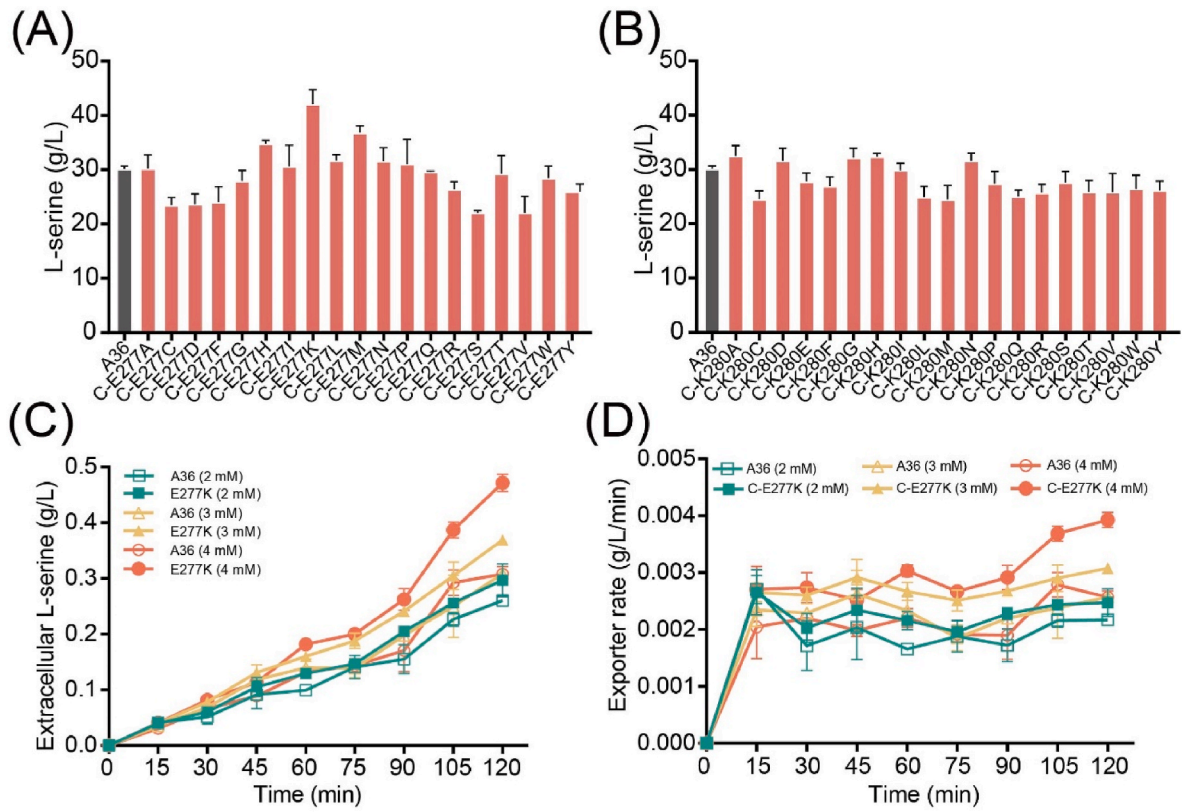

Fig. 4. L-serine production of strain A36 and its mutants. (A) The L-serine titer of E277 mutant strain and A36. (B) The L-serine titer of K280 mutant strain and A36. (C) Time courses of extracellular concentrations of L-serine. (D) Time courses of L-serine exporter rate. (green: 2 mM Ser-Ser; yellow: 3 mM Ser-Ser; red: 4 mM Ser-Ser).

of 8.7 Å, whereas SerE did not reach equilibrium during the simulation. Root mean square fluctuation (RMSF) is used to quantify how much each atom or residue in a molecule fluctuates around its average position. A higher RMSF value indicates that the part has a higher flexibility during the simulation, while a lower RMSF value indicates that the region is more stable. RMSF revealed that $SerE^{E277K}$ exhibited less fluctuation compared to the wild type, indicating a more stable protein structure. This higher stability likely contributed to stronger interactions between L-serine and protein residues, resulting in improved export efficiency.

The binding energy of L-serine to both wild type and mutant $SerE^{E277K}$ was evaluated. The mutant $SerE^{E277K}$ exhibited a lower binding energy of -7.22 ± 2.90 kcal/mol, indicating that the mutation enhanced the binding affinity for L-serine (Table 3). The number, size and strength of hydrogen bonds were analyzed to further understand the binding interactions (Fig. 5D). The mutant $SerE^{E277K}$ formed more hydrogen bonds with L-serine and exhibited better bond density compared to the wild type, indicating more stable binding during the simulation period. Additionally, the mutation of SerE at site 277 from glutamate to lysine reduced the binding energy, and the binding energy of nine other amino acid also (Fig. 5E). This suggests that the mutation facilitated easier binding of L-serine to the exporter.

3.5. Improving L-serine production of mutant strain C-E277K

To further improve L-serine titer of the mutant strain C-E277K, fermentation optimization was conducted. Firstly, the culture conditions for the strain, including liquid loading volume, inoculation amount, and shaking speed, were optimized individually. The optimal fermentation conditions were performed in a 250 mL flask (with 20 mL medium), inoculation amount of 4% and shaking speed of 140 rpm (Fig. 6A).

Then the fermentation medium was optimized by Bayesian optimization. In our previous studies, we have carefully studied the medium components of the strain A36, and found that five factors were beneficial for cell growth and L-serine production. So we optimized these five factors. After the testing of the initial settings of 5 components (Table 4, index 1–20), another 2 rounds of Bayesian optimization were performed. The first round eliminated 4 similar settings and the results (Table 4, index 21–23) showed no improvements, while the second round eliminated 2 similar settings and the results (Table 4, index 24–28) showed relatively high yields. The hyperparameters' likelihood and the candidates' probability of improvement reached their maximum in both rounds. And this guaranteed the reliability of the Gaussian process and the candidates. The optimization was terminated because the suggested candidates of the third round was similar to the those of the second round. According to the model results, the maximum L-serine titer was estimated to be 45.05 g/L under the following conditions: sucrose 120 g/L, $(NH_4)_2SO_4$ 39.8 g/L, $MgSO_4{\cdot}7H_2O$ 0.4 g/L, PCA 26.5 mg/L, and biotin 71.2 μg/L (Fig. 6B).

The mutant strain C-E277K was fermented under the optimized medium in 5-L bioreactor. The results showed rapid cell growth and sucrose consumption within the first 60 h (Fig. 6C). Subsequently, cell growth stabilized, and L-serine titer began to increase sharply at 72 h, reaching a final titer of 47.77 g/L with a productivity of 0.4 g/(L·h). And L-serine titer increased by 13.5% after optimization. This represents the highest reported L-serine titer achieved in *C. glutamicum* through direct fermentation.

4. Discussion

Amino acids exporter is crucial for improving their production in *C. glutamicum*. To date, seven exporters have been identified for the export of 13 amino acids in *C. glutamicum*, [10,36–41]. Zhou introduced a designed Lysine-ON ribose switch into the *lysE* (encoding lysine exporter) of *C. glutamicum* LPECRS, achieving dynamic control of

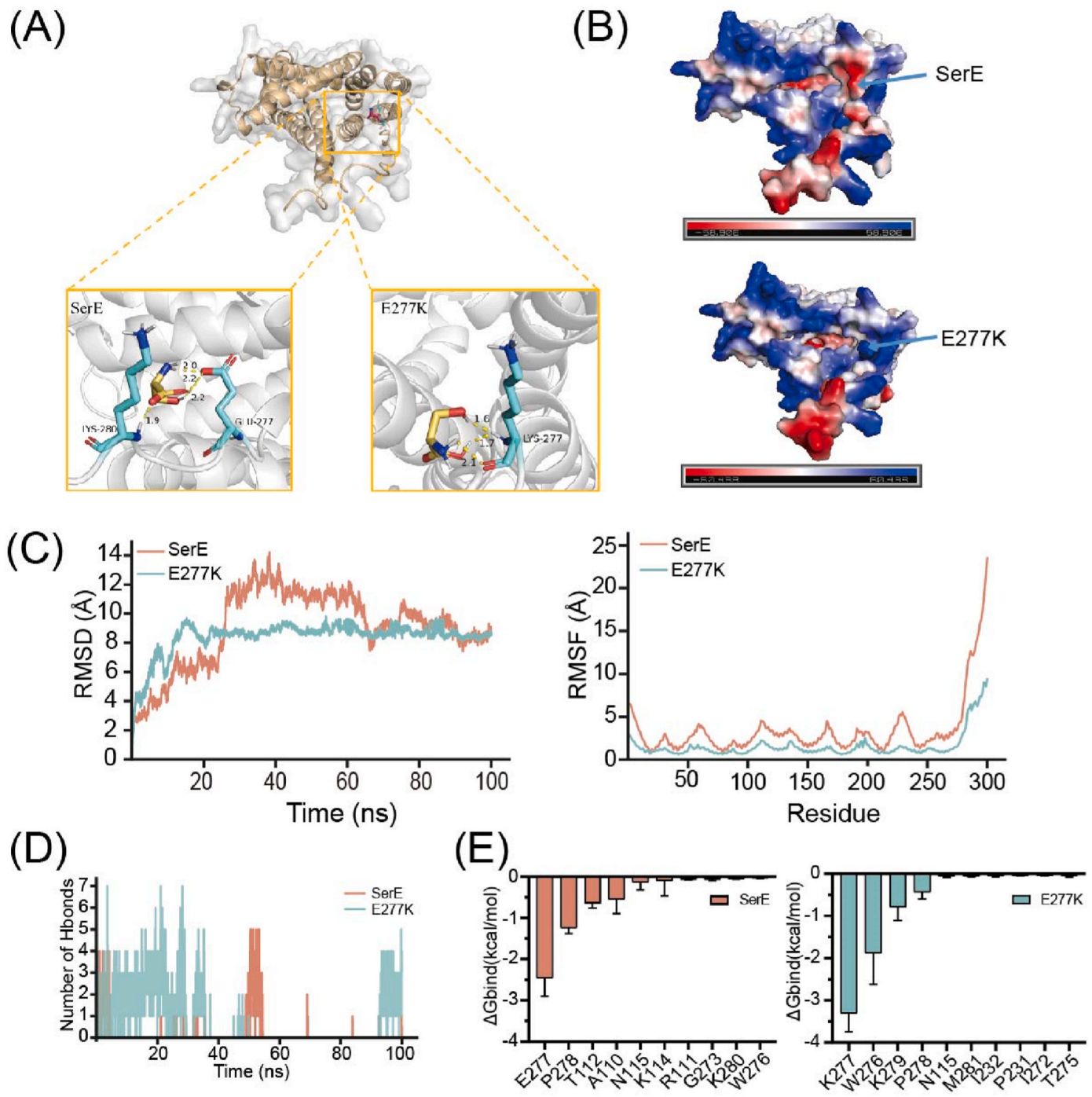

Fig. 5. Structure and molecular dynamics analysis of SerE and the mutant SerE^{E277K}. (A) Intramolecular interaction of mutant SerE^{E277K} and wild type with ligand. (B) Surface charge analysis of mutant SerE^{E277K} and wild-type (red: positive electrostatic potential region, blue: negative electrostatic potential region). (C) Molecular dynamics simulation results for mutant SerE^{E277K} and wild-type. (D) Changes in the number of hydrogen bonds between ligand and protein during the simulation. (E) Binding energy of top 10 amino acids that make an important contribution between ligand and protein during the simulation.

Table 3
Binding free energies and energy components predicted by MM/GBSA (kcal/mol).

exporter	ΔE_{vdw}	ΔE_{elec}	ΔG_{GB}	ΔG_{GB}	ΔG_{bind}
SerE	−9.78 ± 1.53	−24.14 ± 3.68	31.42 ± 3.13	−1.44 ± 0.04	−3.95 ± 1.12
SerE^{E277K}	−5.68 ± 0.74	−48.74 ± 10.65	48.79 ± 8.00	−1.57 ± 0.23	−7.22 ± 2.90

ΔE_{vdW}: van der Waals energy. ΔE_{elec}: electrostatic energy. ΔG_{GB}: electrostatic contribution to solvation. ΔG_{SA}: non-polar contribution to solvation. ΔG_{bind}: binding free energy.

Table 4
Optimization of fermentation medium based on Bayesian models.

Culture-medium number	Sucrose (g/L)	$(NH_4)_2SO_4$ (g/L)	$MgSO_4·7H_2O$ (g/L)	PCA (mg/L)	Biotin (μg/L)
Control	100	30	0.5	30	50
1	80	15	0.4	45	50
2	80	30	0.2	15	75
3	80	30	0.2	30	25
4	80	45	0	45	25
5	80	45	0.2	45	25
6	100	30	0	15	25
7	100	30	0	15	75
8	100	30	0.4	15	50
9	100	45	0	45	75
10	100	45	0.2	30	50
11	100	45	0.4	30	50
12	120	15	0.4	45	75
13	120	15	0.6	15	25
14	120	15	0.6	15	50
15	120	30	0	45	50
16	120	30	0.2	15	50
17	120	30	0.2	30	75
18	120	30	0.6	45	50
19	120	45	0.6	15	75
20	120	45	0.6	30	75
21	80.01	15.01	0.60	15.01	74.99
22	95.30	38.17	0.05	30.28	49.13
23	83.83	26.89	0.04	18.34	67.08
24	120.0	45.0	0.2	45.0	25.0
25	120.0	32.0	0.5	42.7	53.8
26	120.0	39.8	0.4	26.5	71.2
27	120.0	30.1	0.6	44.6	51.0
28	83.8	26.9	0.0	18.3	67.1

L-lysine export and increasing the L-Lysine titer by 21% [42]. Similarly, Zhang enhanced LysE expression in *C. glutamicum* S9114, resulting in a 21.8% increase in L-ornithine titer to 18.4 g/L [14]. Additionally, the L-glutamate exporter $MscCG_2$ was modified through protein engineering, combining with the directed evolution and computer-aided design to achieve a 1.5-fold increase in L-glutamate titer [43]. Although exporters in *C. glutamicum* have been studied to increase amino acid production [44,45], no studies focused on modifying L-serine exporter to improve L-serine export.

In this study, we explored the effects of overexpressing and deleting the L-serine exporter SerE on cell growth and L-serine titer *in C. glutamicum*. Notably, SerE overexpression in strain A36 increased the L-serine titer by 15.1%, but reduced cell growth. This may be due to the importance of L-serine for cell growth, and SerE overexpression using constitutive promoters led to more L-serine transport out of the cell, resulting in insufficient L-serine required for cell growth. In addition, overexpression of the membrane protein often leads to severe growth inhibition, as seen in the reduced biomass of plasmid-based overexpression strains, similar to findings by Wagner et al. [46]. For the SerE deletion strain A36Δ*serE*, the growth rate was initially rapid but slowed later, we speculated that the L-serine synthesized in the early stage was not transported out of the cell and was fully used for cell growth. After SerE deletion, intracellular L-serine accumulated, but purine content decreased, deteriorating cell growth [47]. In addition, we suspected that that L-serine could be reimported through the L-serine uptake system, thus hampering L-serine production [48]. Therefore, enhancing the export capacity of SerE is critical for L-serine production. In the future, we will further focus on the uptake pathway of L-serine.

To improve the export capacity of SerE, we used computer-aided design to model and analyze SerE's structure, found that the E277 site is located in the cytoplasmic region at the end of the exporter, unlike other exporters whose substrate-binding sites are located in the transmembrane region. We hypothesize that this terminal region may affect substrate accessibility and affinity by altering the protein's spatial conformation. Based on the inward-facing state model of SerE and studies on the DMT superfamily's common export mechanism [37], and the structure-function analysis of YddG [49], we propose that L-serine binding induces a conformational change that opens the pathway to the cell exterior, increasing L-serine export. Future work will focus on

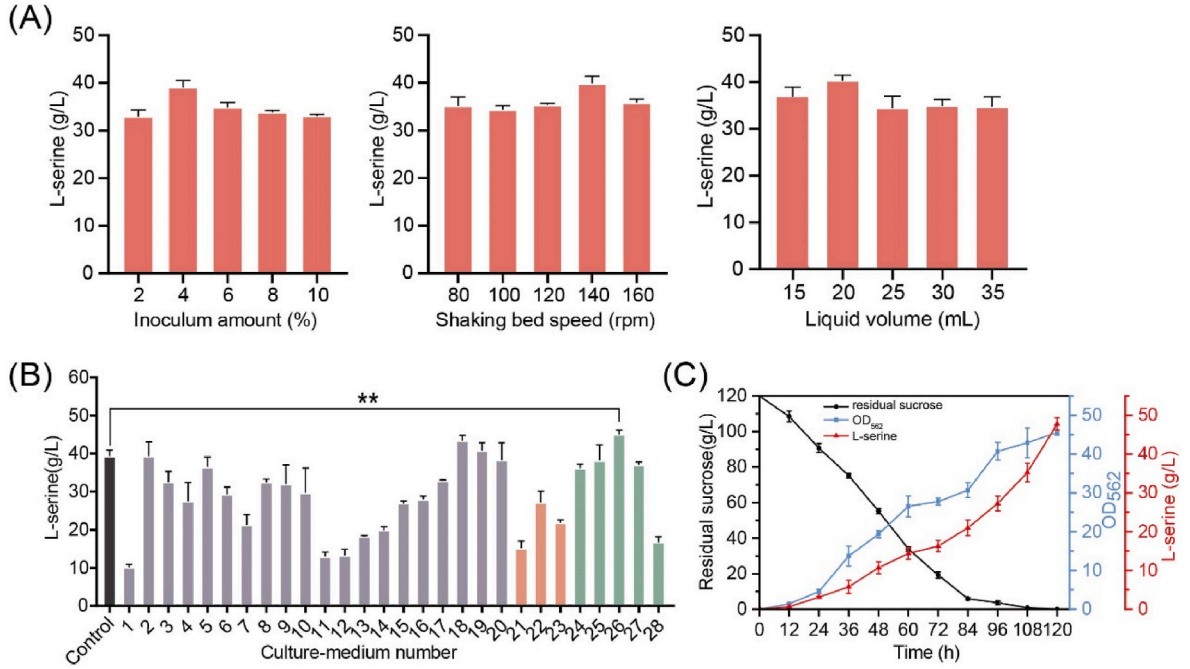

Fig. 6. Fermentation optimization of strain C-E277K. (A) Impact of varying inoculations on production by *C. glutamicum* C-E277K during fermentation. Impact of varying shaker speed on production by *C. glutamicum* C-E277K during fermentation. Impact of varying liquid loading on production by *C. glutamicum* C-E277K during fermentation. (B) Influence of different concentration medium on L-serine titer of *C. glutamicum* C-E277K during fermentation (Control: Gray, group 1–20: purple, group 21–23: orange, group 24–28: green). (C) Fermentation results for the strain C-E277K under optimal conditions in a 5-L bioreactor. The cell growth (blue), L-serine titer (red), and residual sucrose (black) of strain C-E277K are presented.

elucidating the substrate export mechanism of SerE.

After selecting a successfully modified SerE mutant, we evaluated its L-serine export capacity using an amino acid export assay. The export capacity of mutant C-E277K increased by 53.2%. However, adding 3 mM and 4 mM Ser-Ser had little effect on the parent strain A36's export capacity at 120 min, while mutant strain increased by 27.7%. Site 277 of SerE is acidic amino acid before mutation and becomes an alkaline amino acid after mutation. Replacing hydrophilic glutamic acid with lysine aligns with the surrounding amino acid's charge distribution, potentially explaining the favorable electrostatic charge changes in the E277K mutant [50]. The shortened hydrogen bond spacing in E277K enhanced the protein's structural rigidity, which may contribute to its increased stability. MD simulations revealed that E277K exhibited steadier RMSD and lower RMSF values compared to the wild type, indicating enhanced structural rigidity and stability [51].

In this study, the medium of the mutant strain C-E277K was optimized by Bayesian optimization, reaching its highest titer of 47.77 g/L. Dealing with the input of 5 factors, factorial design demands at least $2^5 = 32$ settings to model and optimize within a round. This number is nearly closed to the total number of the tests in this study, which demonstrates the efficiency of the adopted Bayesian optimization. Also, the need of the design is just to be representative instead of be strictly limited to low-level, high-level or central point, and the design can be directed to the interesting domain of the input space. Further, data of similar strain could also be utilized in Bayesian optimization. For example, Xiao used Bayesian optimization to increase S-adenosyl-L-methionine titer by 26.3-fold [35]. Thompson et al. developed a physically-constrained recurrent neural network and combined it with Bayesian experimental design to optimize the operating conditions of a bioreactor for microbial communities [18,52]. In all, Bayesian optimization guarantees the flexibility, time- and cost-efficiency when applied in the optimization of the fermentation condition.

5. Conclusion

In this study, we successfully developed a mutant (C-E277K) of L-serine exporter SerE through rational computer-aided design and bioinformatics analysis. The mutant exhibited a 53.2% increase in export capacity compared to the wild-type SerE, resulting in a 39.6% increase in L-serine titer. Structural analysis and molecular dynamics simulation were employed to elucidate the mechanisms underlying the enhanced performance of this mutant. Furthermore, Bayesian optimization was applied to improve L-serine titer of mutant C-E277K, leading to an L-serine titer of 47.77 g/L. This represents the highest reported L-serine titer achieved using *C. glutamicum*. This study provides valuable insights for improving L-serine and other high-value amino acids production.

CRediT authorship contribution statement

Yifan Huang: Writing – original draft, Methodology, Investigation, Data curation. **Yujie Gao:** Investigation, Data curation. **Yamin Huang:** Software, Investigation. **Xiaogang Wang:** Software, Methodology. **Meijuan Xu:** Resources, Methodology. **Guoqiang Xu:** Supervision, Resources, Project administration. **Xiaojuan Zhang:** Supervision, Resources, Project administration. **Hui Li:** Supervision, Resources, Project administration. **Jinsong Shi:** Supervision, Resources, Project administration. **Zhenghong Xu:** Resources, Funding acquisition. **Xiaomei Zhang:** Writing – review & editing, Supervision, Project administration, Funding acquisition.

Declaration of competing interests

All the authors declare that they have no competing interests.

Acknowledgment

This work was supported by the National Natural Science Foundation of China (32171470).

References

[1] Giacomini KM, Huang S-M, Tweedie DJ, Benet LZ, Brouwer KL, Chu X, et al. Membrane transporters in drug development. Nat Rev Drug Discov 2010;9(3):215–36. https://doi.org/10.1038/nrd3028.
[2] Zhang X, Xu G, Shi J, Koffas MAG, Xu Z. Microbial production of L-serine from renewable feedstocks. Trends Biotechnol 2018;36(7):700–12. https://doi.org/10.1016/j.tibtech.2018.02.001.
[3] Teng Z, Pan X, Liu Y, You J, Zhang H, Zhao Z, et al. Engineering serine hydroxymethyltransferases for efficient synthesis of L-serine in *Escherichia coli*. Bioresour Technol 2024;393:130153. https://doi.org/10.1016/j.biortech.2023.130153.
[4] Chen Z, Zhou P, Zhao Z, Li B. Enhanced production of L-serine in *Escherichia coli* by fermentation process optimization and transcriptome sequencing. Biochem Eng J 2023;200:109109. https://doi.org/10.1016/j.bej.2023.109109.
[5] Mundhada H, Schneider K, Christensen HB, Nielsen AT. Engineering of high yield production of L-serine in *Escherichia coli*. Biotechnol Bioeng 2016;113(4):807–16. https://doi.org/10.1002/bit.25844.
[6] Li Y, Chen GK, Tong XW, Zhang HT, Liu XG, Liu YH, et al. Construction of *Escherichia coli* strains producing L-serine from glucose. Biotechnol Lett 2012;34(8):1525–30. https://doi.org/10.1007/s10529-012-0937-0.
[7] Peters-Wendisch P, Stolz M, Etterich H, Kennerknecht N, Sahm H, Eggeling L. Metabolic engineering of *Corynebacterium glutamicum* for L-serine production. Appl Environ Microbiol 2005;71(11):7139–44. https://doi.org/10.1128/aem.71.11.7139-7144.2005.
[8] Stolz M, Peters-Wendisch P, Etterich H, Gerharz T, Faurie R, Sahm H, et al. Reduced folate supply as a key to enhanced L-serine production by *Corynebacterium glutamicum*. Appl Environ Microbiol 2007;73(3):750–5. https://doi.org/10.1128/aem.02208-06.
[9] Rennig M, Mundhada H, Wordofa GG, Gerngross D, Wulff T, Worberg A, et al. Industrializing a bacterial strain for L-serine production through translation initiation optimization. ACS Synth Biol 2019;8(10):2347–58. https://doi.org/10.1021/acssynbio.9b00169.
[10] Zhang X, Gao Y, Chen Z, Xu G, Zhang X, Li H, et al. High-yield production of L-serine through a novel identified exporter combined with synthetic pathway in *Corynebacterium glutamicum*. Microb Cell Fact 2020;19:1–14. https://doi.org/10.1186/s12934-020-01374-5.
[11] Zhu Q, Zhang X, Luo Y, Guo W, Xu G, Shi J, et al. L-Serine overproduction with minimization of by-product synthesis by engineered *Corynebacterium glutamicum*. Appl Microbiol Biotechnol 2015;99(4):1665–73. https://doi.org/10.1007/s00253-014-6243-0.
[12] Eggeling L. Exporters for production of amino acids and other small molecules. Adv Biochem Eng Biotechnol 2017;159:199–225. https://doi.org/10.1007/10_2016_32.
[13] Jones CM, Hernández Lozada NJ, Pfleger BF. Efflux systems in bacteria and their metabolic engineering applications. Appl Microbiol Biotechnol 2015;99(22):9381–93. https://doi.org/10.1007/s00253-015-6963-9.
[14] Zhang B, Yu M, Zhou Y, Li Y, Ye BC. Systematic pathway engineering of *Corynebacterium glutamicum* S9114 for L-ornithine production. Microb Cell Fact 2017;16(9):1–10. https://doi.org/10.1186/s12934-017-0776-8.
[15] Gao Y, Zhang X, Xu G, Zhang X, Li H, Shi J, et al. Enhanced L-serine production by *Corynebacterium glutamicum* based on novel insights into L-serine exporters. J Biotechnol 2024;19(1):2300136. https://doi.org/10.1002/biot.202300136.
[16] Montgomery DC. Design and analysis of experiments. tenth ed. Hoboken, NJ: John Wiley & Son; 2017.
[17] Yoshida K, Watanabe K, Chiou TY, Konishi M. High throughput optimization of medium composition for *Escherichia coli* protein expression using deep learning and Bayesian optimization. J Biosci Bioeng 2023;135(2):127–33. https://doi.org/10.1016/j.jbiosc.2022.12.004.
[18] Gisperg F, Klausser R, Elshazly M, Kopp J, Brichtová EP, Spadiut O. Bayesian optimization in bioprocess engineering-where do we stand today? Biotechnol Bioeng 2025. https://doi.org/10.1002/bit.28960.
[19] van der Rest ME, Lange C, Molenaar D. A heat shock following electroporation induces highly efficient transformation of *Corynebacterium glutamicum* with xenogeneic plasmid DNA. Appl Microbiol Biotechnol 1999;52(4):541–5. https://doi.org/10.1007/s002530051557.
[20] Xu D, Tan Y, Shi F, Wang X. An improved shuttle vector constructed for metabolic engineering research in *Corynebacterium glutamicum*. Plasmid 2010;64(2):85–91. https://doi.org/10.1016/j.plasmid.2010.05.004.
[21] Schäfer A, Tauch A, Jäger W, Kalinowski J, Thierbach G, Pühler A. Small mobilizable multi-purpose cloning vectors derived from the *Escherichia coli* plasmids pK18 and pK19: selection of defined deletions in the chromosome of *Corynebacterium glutamicum*. Gene 1994;145(1):69–73. https://doi.org/10.1016/0378-1119(94)90324-7.
[22] Thieker DF, Maguire JB, Kudlacek ST, Leaver-Fay A, Lyskov S, Kuhlman B. Stabilizing proteins, simplified: a Rosetta-based webtool for predicting favorable mutations. Protein Sci 2022;31(10):e4428. https://doi.org/10.1002/pro.4428.

[23] Simic P, Sahm H, Eggeling L. L-threonine export: use of peptides to identify a new translocator from *Corynebacterium glutamicum*. J Bacteriol 2001;183(18):5317–24. https://doi.org/10.1128/JB.183.18.5317-5324.2001.
[24] Erdmann A, Weil B, Kramer R. Lysine secretion by wild-type *Corynebacterium glutamicum* triggered by dipeptide uptake. J Gen Microbiol 1993;139:3115–22. https://doi.org/10.1099/00221287-139-12-3115.
[25] Keilhauer C, Eggeling L, Sahm H. Isoleucine synthesis in *Corynebacterium glutamicum*: molecular analysis of the *ilvB-ilvN-ilvC* operon. J Bacteriol 1993;175 (17):5595–603. https://doi.org/10.1128/jb.175.17.5595-5603.1993.
[26] Liu Q, Liang Y, Zhang Y, Shang X, Liu S, Wen J, et al. YjeH is a novel exporter of L-methionine and branched-chain amino acids in *Escherichia coli*. Appl Environ Microbiol 2015;81(22):7753–66. https://doi.org/10.1128/aem.02242-15.
[27] Jumper J, Evans R, Pritzel A, Green T, Figurnov M, Ronneberger O, et al. Highly accurate protein structure prediction with AlphaFold. Nature 2021;596(7873): 583–9. https://doi.org/10.1038/s41586-021-03819-2.
[28] Morris GM, Huey R, Lindstrom W, Sanner MF, Belew RK, Goodsell DS, et al. AutoDock4 and AutoDockTools4: automated docking with selective receptor flexibility. J Comput Chem 2009;30(16):2785–91. https://doi.org/10.1002/jcc.21256.
[29] Salomon-Ferrer R, Case DA, Walker RC. An overview of the amber biomolecular simulation package. Wires Comput Mol Sci 2013;3(2):198–210. https://doi.org/10.1002/wcms.1121.
[30] Maier JA, Martinez C, Kasavajhala K, Wickstrom L, Hauser KE, Simmerling C. ff14SB: improving the accuracy of protein side chain and backbone parameters from ff99SB. J Chem Theor Comput 2015;11(8):3696–713. https://doi.org/10.1021/acs.jctc.5b00255.
[31] Wang J, Wolf RM, Caldwell JW, Kollman PA, Case DA. Development and testing of a general amber force field. J Comput Chem 2004;25(9):1157–74. https://doi.org/10.1002/jcc.20035.
[32] Mark P, Nilsson L. Structure and dynamics of the TIP3P, SPC, and SPC/E water models at 298 K. J Phys Chem A 2001;105(43):9954–60. https://doi.org/10.1021/jp003020w.
[33] Fedorchuk TP, Khusnutdinova AN, Flick R, Yakunin AF. Site-directed mutagenesis and stability of the carboxylic acid reductase MAB4714 from *Mycobacterium abscessus*. J Biotechnol 2019;303:72–9. https://doi.org/10.1016/j.jbiotec.2019.07.009.
[34] Zhang X, Lai L, Xu G, Zhang X, Shi J, Xu Z. Effects of pyruvate kinase on the growth of *Corynebacterium glutamicum* and L-serine accumulation. Process Biochem 2017; 55:32–40. https://doi.org/10.1016/j.procbio.2017.01.028.
[35] Xiao W, Shi X, Huang H, Wang X, Liang W, Xu J, et al. Enhanced synthesis of S-adenosyl-L-methionine through combinatorial metabolic engineering and Bayesian optimization in *Saccharomyces cerevisiae*. Biotechnol J 2024;19(3):e2300650. https://doi.org/10.1002/biot.202300650.
[36] Kennerknecht N, Sahm H, Yen MR, Pátek M, Saier Jr Jr MH, Eggeling L. Export of L-isoleucine from *Corynebacterium glutamicum*: a two-gene-encoded member of a new translocator family. J Bacteriol 2002;184(14):3947–56. https://doi.org/10.1128/jb.184.14.3947-3956.2002.
[37] Trötschel C, Deutenberg D, Bathe B, Burkovski A, Krämer R. Characterization of methionine export in *Corynebacterium glutamicum*. J Bacteriol 2005;187(11): 3786–94. https://doi.org/10.1128/jb.187.11.3786-3794.2005.
[38] Nakamura J, Hirano S, Ito H, Wachi M. Mutations of the *Corynebacterium glutamicum ncgl1221* gene, encoding a mechanosensitive channel homolog, induce L-glutamic acid production. Appl Environ Microbiol 2007;73(14):4491–8. https://doi.org/10.1128/aem.02446-06.
[39] Eggeling L, Sahm H. New ubiquitous translocators: amino acid export by *Corynebacterium glutamicum* and *Escherichia coli*. Arch Microbiol 2003;180(3): 155–60. https://doi.org/10.1007/s00203-003-0581-0.
[40] Vrljic M, Sahm H, Eggeling L. A new type of transporter with a new type of cellular function: L-lysine export from *Corynebacterium glutamicum*. Mol Microbiol 1996;22 (5):815–26. https://doi.org/10.1046/j.1365-2958.1996.01527.x.
[41] Simic P, Willuhn J, Sahm H, Eggeling L. Identification of *glyA* (encoding serine hydroxymethyltransferase) and its use together with the exporter ThrE to increase L-threonine accumulation by *Corynebacterium glutamicum*. Appl Environ Microbiol 2002;68(7):3321–7. https://doi.org/10.1128/aem.68.7.3321-3327.2002.
[42] Zhou LB, Zeng AP. Engineering a lysine-ON riboswitch for metabolic control of lysine production in *Corynebacterium glutamicum*. ACS Synth Biol 2015;4(12): 1335–40. https://doi.org/10.1021/acssynbio.5b00075.
[43] Nie Z, Liu P, Wang Y, Guo X, Tan Z, Shen J, et al. Directed evolution and rational design of mechanosensitive channel MscCG2 for improved glutamate excretion efficiency. J Agric Food Chem 2021;69(51):15660–9. https://doi.org/10.1021/acs.jafc.1c07086.
[44] Huhn S, Jolkver E, Krämer R, Marin K. Identification of the membrane protein SucE and its role in succinate transport in *Corynebacterium glutamicum*. Appl Microbiol Biotechnol 2011;89:327–35. https://doi.org/10.1007/s00253-010-2855-1.
[45] Wang Y, Cao G, Xu D, Fan L, Wu X, Ni X, et al. A novel *Corynebacterium glutamicum* L-glutamate exporter. Appl Environ Microbiol 2018;84(6). https://doi.org/10.1128/aem.02691-17. e02691-17.
[46] Wagner S, Baars L, Ytterberg AJ, Klussmeier A, Wagner CS, Nord O, et al. Consequences of membrane protein overexpression in *Escherichia coli*. Mol Cell Proteomics 2007;6(9):1527–50. https://doi.org/10.1074/mcp.M600431-MCP200.
[47] Zhang Y, Shang X, Lai S, Zhang Y, Hu Q, Chai X, et al. Reprogramming one-carbon metabolic pathways to decouple L-serine catabolism from cell growth in *Corynebacterium glutamicum*. ACS Synth Biol 2018;7(2):635–46. https://doi.org/10.1021/acssynbio.7b00373.
[48] Wang C, Wu J, Shi B, Shi J, Zhao Z. Improving L-serine formation by *Escherichia coli* by reduced uptake of produced L-serine. Microb Cell Fact 2020;19(1):66. https://doi.org/10.1186/s12934-020-01323-2.
[49] Tsuchiya H, Doki S, Takemoto M, Ikuta T, Higuchi T, Fukui K, et al. Structural basis for amino acid export by DMT superfamily transporter YddG. Nature 2016;534 (7607):417–20. https://doi.org/10.1038/nature17991.
[50] Cui Y, Yang M, Liu N, Wang S, Sun Y, Sun G, et al. Computer-aided rational design strategy to improve the thermal stability of alginate lyase AlyMc. J Agric Food Chem 2024;72(6):3055–65. https://doi.org/10.1021/acs.jafc.3c07215.
[51] Badieyan S, Bevan DR, Zhang C. Study and design of stability in GH5 cellulases. Biotechnol Bioeng 2012;109(1):31–44. https://doi.org/10.1002/bit.23280.
[52] Thompson JC, Zavala VM, Venturelli OS. Integrating a tailored recurrent neural network with Bayesian experimental design to optimize microbial community functions. PLoS Comput Biol 2023;19(9):e1011436. https://doi.org/10.1371/journal.pcbi.1011436.
[53] Xu D, Tan Y, Li Y, Wang X. Construction of a novel promoter-probe vector and its application for screening strong promoter for *Brevibacterium flavum* metabolic engineering. World J Microbiol Biotechnol 2011;27:961–8. https://doi.org/10.1007/s11274-010-0539-8.